

This document is confidential and is proprietary to the American Chemical Society and its authors. Do not copy or disclose without written permission. If you have received this item in error, notify the sender and delete all copies.

Macroscopic Differentiators for Microscopic Structural Non-ideality in Binary Ionic Liquid Mixtures

Journal:	<i>The Journal of Physical Chemistry</i>
Manuscript ID	Draft
Manuscript Type:	Article
Date Submitted by the Author:	n/a
Complete List of Authors:	Kapoor, Utkarsh; University of Delaware, Chemical and Biomolecular Engineering Shah, Jindal; Oklahoma State University Stillwater, Chemical Engineering

SCHOLARONE™
Manuscripts

1
2
3
4
5
6
7
8
9 **Macroscopic Differentiators for Microscopic**
10
11 **Structural Non-ideality in Binary Ionic Liquid**
12
13
14
15
16 **Mixtures**
17
18
19

20 Utkarsh Kapoor^{†,‡} and Jindal K. Shah^{*,†}
21
22

23 *†School of Chemical Engineering, Oklahoma State University, Stillwater, Oklahoma 74078,
24 United States*

25 *‡Current address: Department of Chemical and Biomolecular Engineering, Colburn
26 Laboratory, University of Delaware, Newark, Delaware 19716, United States*

27
28
29
30 E-mail: jindal.shah@okstate.edu
31
32
33
34
35
36
37
38
39
40
41
42
43
44
45
46
47
48
49
50
51
52
53
54
55
56
57
58
59
60

Abstract

Combining two ionic liquids to form a binary ionic liquid mixture is a simple yet effective strategy to not only expand the number of ionic liquids but also precisely control various physicochemical properties of resultant ionic liquid mixtures. From a fundamental thermodynamic point of view, it is not entirely clear whether such mixtures can be classified as ideal solutions. Given a large number of binary ionic liquid mixtures that emerge, the ability to predict the presence of non-ideality in such mixtures *a priori* without the need for experimentation or molecular simulation-based calculations is immensely valuable for their rational design. In this research report, we demonstrate that the difference in the molar volumes (ΔV) of the pure ionic liquids and the difference in the hydrogen bonding ability of anions ($\Delta\beta$) are the primary determinants of non-ideal behavior of binary ionic liquid mixtures containing a common cation and two anions. Our conclusion is derived from a comparison of microscopic structural properties expressed in terms of radial, spatial, and angular distributions for binary mixtures and those of the corresponding pure ionic liquids. Molecular dynamics simulations of sixteen binary ionic liquid mixtures, containing a common cation 1-*n*-butyl-3-methylimidazolium $[\text{C}_4\text{mim}]^+$ and combinations of (less basic) fluorinated {trifluoromethylacetate $[\text{TFA}]^-$, trifluoromethanesulfonate $[\text{TFS}]^-$, bis(trifluoromethanesulfonyl)imide $[\text{NTf}_2]^-$, and tris (pentafluoroethyl) trifluorophosphate $[\text{eFAP}]^-$ } vs. (more basic) non-fluorinated {chloride Cl^- , acetate $[\text{OAC}]^-$, methylsulfate $[\text{MeSO}_4]^-$, and dimethyl phosphate $[\text{Me}_2\text{PO}_4]^-$ } anions, were conducted. The large number of binary ionic liquid mixtures examined here enabled us to span a broad range of ΔV and $\Delta\beta$ values. The results indicate that binary mixtures of two ionic liquids for which $\Delta V > 60 \text{ cm}^3/\text{mol}$ and $\Delta\beta > 0.4$ are expected to be microscopically non-ideal. On the other hand, $\Delta V < 60 \text{ cm}^3/\text{mol}$ and $\Delta\beta < 0.4$ will lead to molecular structures that are not differentiated from those of their pure ionic liquid counterparts.

1 2 3 4 5 6 7 8 9 10 11 12 13 14 15 16 17 18 19 20 21 22 23 24 25 26 27 28 29 30 31 32 33 34 35 36 37 38 39 40 41 42 43 44 45 46 47 48 49 50 51 52 53 54 55 56 57 58 59 60 Introduction

Ionic liquids are an intriguing class of molten salts, which are composed of molecular ions the asymmetry of which results in packing frustration leading to their melting points below 100°C. At molecular level, ionic liquids are characterized by a delicate balance of Coulombic, dispersion, hydrogen bonding, and π - π interactions giving rise to properties such as negligible vapor pressure and solvation of polar and non-polar solutes. A natural way of manipulating these interactions to obtain ionic liquids with improved properties is by changing the cation, anion or both. Due to the diversity of available ions, such approach has been the primary focus to design ionic liquids with desired properties resulting in a large number of ionic liquids synthesized till date. As an illustration, the ILThermo Database maintained by the National Institute for Standard and Technology contains physicochemical properties of 1400 unique ionic liquids. In lieu of synthesizing new ionic moieties, mixing of two ionic liquids is probably the simplest and cost-effective strategy to generate new ionic liquids in which molecular-level interactions governing macroscopic properties are modified.¹⁻⁸ Considering that the mole fractions of the constituent ionic liquids can be varied almost continuously, the approach holds great promise to produce a large number of ionic liquids increasing the probability of discovering ionic liquids with desired properties. However, due to the combinatorics, the number of potential ionic liquid becomes too large to be studied rapidly either experimentally or with molecular simulations. To navigate a large chemical space comprised of potentially 10^{18} ionic liquids,⁹ it is imperative that a first-pass, rapid, robust, easy-to-use screen based entirely on the properties of pure ionic liquid be developed to differentiate ideal vs. non-ideal ionic liquid mixtures.

While results from several studies indicate that thermodynamic properties such as enthalpy and chemical potential, or volumetric properties such as excess molar volumes obey ideal mixing law, there exist ionic liquid mixtures exhibiting non-ideal behavior. The ideal behavior is generally explained in terms of the similarity between interactions in the mixture

1
2
3 and pure ionic liquids. On the other hand, changes in one or more molecular level interac-
4 tions with respect to those present in pure ionic liquids have been invoked to rationalize the
5 non-ideal behavior. The origin of such non-ideality has been suggested to be rooted in the
6 differences in the anion size/ionic liquid molar volumes and the hydrogen bond ability (β) of
7 anions. For example, binary ionic liquid mixtures containing anions with a very substantial
8 difference in β parameter have been reported to yield non-ideal behavior in terms of excess
9 molar volumes, viscosity, conductivity, and glass transition temperature experiments.^{1,2,10}
10 Our work and that of others have also shown that when binary ionic liquid mixtures with
11 a common cation and two anions with a large difference in the hydrogen bond ability are
12 formed, the molecular arrangement of anions around the cation in the mixture can markedly
13 differ from those in the pure ionic liquids.¹¹ We have also demonstrated that the presence of
14 “non-native” arrangements of anions exert a profound influence on the physical dissolution
15 mechanism of CO₂ at molecular level.¹²
16
17
18
19
20
21
22
23
24
25
26
27
28
29
30

31 Despite the significance of molar volumes and hydrogen bond ability of the anions in pre-
32 dicting the non-ideal behavior in ionic liquid mixtures, it is surprising that a systematic
33 investigation evaluating the influence of these markers has been absent in the literature.
34 In the present work, we resort to molecular dynamics simulations to assess the ability of
35 these two descriptors in providing clues to the non-ideality in binary ionic liquid mixtures.
36 We report a comparison of molecular arrangements for a total of sixteen binary ionic liquid
37 mixture systems containing the common cation 1-*n*-butyl-3-methylimidazolium [C₄mim]⁺
38 and mixtures of (less basic, low β values) fluorinated {trifluoroacetate [TFA]⁻, trifluorosul-
39 fonate [TFS]⁻, bis(trifluoromethanesulfonyl)imide [NTf₂]⁻, and tris(pentafluoroethyl) tri-
40 fluorophosphate [eFAP]⁻} vs. (more basic, high β values) non-fluorinated {chloride Cl⁻,
41 acetate [OAC]⁻, methylsulfate [MeSO₄]⁻, and dimethylphosphate [Me₂PO₄]⁻} anions (see
42 Supporting Information for the molecular structures, β values and molar volumes).
43
44
45
46
47
48
49
50
51
52
53
54
55
56
57
58
59
60

Computational Details

The intra- and inter-molecular interactions were modeled using an all-atom force field developed by Canongia Lopes-Pádua^{13,14} (CL&P) for all the molecules except $[\text{Me}_2\text{PO}_4]^-$ anion, the parameters of which were taken from OPLS-AA force field¹⁵ which has been shown to work well when combined with CL&P parameters.¹⁶⁻¹⁸ The force field has the following functional form:

$$\begin{aligned}
 E_{tot} = & \sum_{ij}^{\text{bonds}} \frac{k_{r,ij}}{2} (r_{ij} - r_{0,ij})^2 + \sum_{ijk}^{\text{angles}} \frac{k_{\theta,ijk}}{2} (\theta_{ijk} - \theta_{0,ijk})^2 \\
 & + \sum_{ijkl}^{\text{torsions}} \sum_{m=1}^4 \frac{k_{m,ijkl}}{2} [1 + (-1)^{m+1} \cos(m\phi_{ijkl})] + \\
 & + \sum_{ij}^{\text{nonbonded}} \left\{ 4\epsilon_{ij} \left[\left(\frac{\sigma_{ij}}{r_{ij}} \right)^{12} - \left(\frac{\sigma_{ij}}{r_{ij}} \right)^6 \right] + \left(\frac{q_i q_j}{r_{ij}} \right) \right\}
 \end{aligned} \quad (1)$$

where $k_{r,ij}$, $k_{\theta,ijk}$, $k_{m,ijkl}$ represent the force constants for bond stretching, angle bending, torsion (both proper and improper), respectively, σ and ϵ denote the size and energy parameter of the 6-12 Lennard-Jones (LJ) potential and q indicate partial charges. As proposed for the force field model, the unlike interactions were computed by the geometric-mean combining rule and 1-4 nonbonded interactions were reduced by a factor of 2 for both LJ and electrostatic interactions. The total charge on the cation and anion is ± 1 . It is worth mentioning that not using either polarizable force field or scaled non-integer charges may be justified as polarizability has minor effect on the local structural properties.¹⁹

Molecular dynamics (MD) simulations were carried out at a temperature and pressure of 353 K and 1 bar using GROMACS 5.1.5 package.^{20,21} Along with pure ionic liquid systems, simulations for a total of five intermediate molar ratios (10:90, 25:75, 50:50, 75:25 and 90:10) obtained by varying the concentrations of the respective anions were performed. With periodic boundary conditions enforced in three dimensions, a system size consisting of 256 ion

1
2
3 pairs was used for all the ionic liquid compositions, except for 10:90 and 90:10 compositions,
4 for which 250 ion pairs were simulated. The simulations were performed in two steps. First,
5 random initial configurations were generated using PACKMOL.²² These initial configura-
6 tions were then subjected to a steepest descent minimization followed by a 2 ns annealing
7 scheme, where the temperature was increased from 353 K to 553 K and then lowered to the
8 desired temperature of 353 K iteratively. Each ionic liquid system was then simulated in
9 canonical (*NVT*) ensemble for a duration of 10 ns, followed by isothermal-isobaric (*NPT*)
10 equilibration run of 20 ns. In second step, the last configuration obtained from the *NPT*
11 equilibration run was used as the initial configuration. This configuration was subjected to
12 the same annealing scheme followed by 10 ns of *NVT*, and 25 ns of *NPT* equilibration and
13 subsequent *NPT* production run of 40 ns. The trajectories obtained from the last 20 ns of
14 the production run, with coordinates were saved every 0.4 ps, were used for the analyses.
15 During the production run, Nosé-Hoover thermostat and Parrinello-Rahman barostat with
16 a coupling time constant of 0.4 ps and 2.0 ps were used to maintain the temperature and
17 pressure. Particle Mesh Ewald (PME) method was used to handle electrostatic interactions
18 while analytical tail corrections were applied for nonbonded LJ interactions, each with a
19 potential cutoff of 16 Å. Since all the fast vibrating modes comprising hydrogen atoms were
20 constraint, the simulations were integrated with a time step of 2 fs. The analysis of the
21 trajectories was performed using TRAVIS package.²³
22
23

43 Results and Discussion

44

45 The systems studied here allowed us to change the values of ΔV (difference in molar vol-
46 umes) and $\Delta\beta$ (difference in the hydrogen bond ability) from low to high systematically,
47 thereby enabling the investigation of difference in entropic and enthalpic contributions in
48 a mixture. The β parameter for all the anions were taken from the works of Spange and
49 co-workers,^{24,25} except for $[\text{Me}_2\text{PO}_4]^-$ and $[\text{eFAP}]^-$, where the β parameters were predicted
50
51
52
53
54
55
56
57
58

1
2
3
4
5
6
7
8
9
10
11
12
13
14
15
16
17
18
19
20
21
22
23
24
25
26
27
28
29
30
31
32
33
34
35
36
37
38
39
40
41
42
43
44
45
46
47
48
49
50
51
52
53
54
55
56
57
58
59
60

1
2
3 using a correlation between β values and calculated hydrogen bond energies suggested by
4 Freire and co-workers.²⁶ Same inferences can also be made using the β parameter values
5 taken from the works of Welton and co-workers²⁷ (see Supporting Information). The molar
6 volumes were predicted from molecular dynamics simulations. Based on these values, we
7 generated Figure 1 displaying (ΔV) and ($\Delta\beta$) of the anions for all the ionic liquid mixtures.
8 Figure 1 depicts four rectangular regions, which can provide guidance in predicting the ideal
9 vs. non-ideal behavior that might be expected for a given binary ionic liquid mixture. In
10 particular, non-ideal mixing behavior in terms of non-native structures (see below) can be
11 expected if the ions comprising the ionic liquid mixture are chosen such that $\Delta V > 60$
12 cm^3/mol and $\Delta\beta > 0.4$ (top right corner of Figure 1 shaded in green) while close to ideal
13 mixing behavior is predicted for the region comprised of $\Delta V < 60 \text{ cm}^3/\text{mol}$ and $\Delta\beta < 0.4$
14 (bottom left corner of Figure 1 shaded in red). As an aside, the data in Figure 1 highlight
15 that though there is a general trend of increasing ΔV and $\Delta\beta$, the correlation is weak at
16 best. As we dive deep into Figure 1 below, we have highlighted several ionic liquids mixtures
17 possessing similar $\Delta\beta$ values and up to a ten-fold variation in ΔV values. Similarly, a two-
18 to three-fold increase in $\Delta\beta$ can be obtained for a given ΔV . In the subsequent sections, we
19 will provide details on how we developed various regions in the master figure and highlight
20 the merit of Figure 1 in predicting the non-ideality of a binary ionic liquid mixture.
21
22
23
24
25
26
27
28
29
30
31
32
33
34
35
36
37
38
39
40
41
42
43
44
45
46
47
48
49
50
51
52
53
54
55
56
57
58
59
60

Non-native structures as a surrogate for non-ideality

In this article, we adopt the differences in the molecular arrangement of anions around the cation between those encountered in a binary ionic liquid mixture and constituent ionic liquids as markers for non-ideality. The choice of this metric is partly due to the difficulty in predicting excess thermodynamic properties for ionic liquid mixtures, such as excess molar volumes and excess enthalpies, which are traditionally invoked to classify ideal vs. non-ideal solutions. The excess quantities tend to be rather small and are sensitive to the selection of a force field model, while the microstructure is more robust. As an evidence, the radial

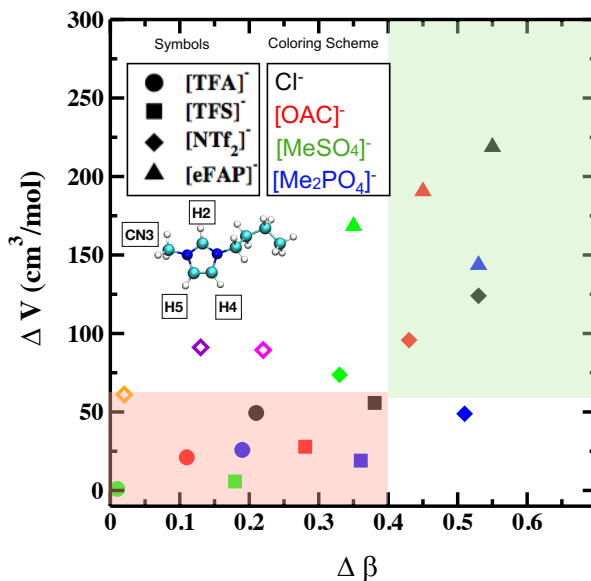


Figure 1: Range of differences in hydrogen bond ability and size / molar volume of anions that leads to non-ideality in 16 binary ionic liquid mixtures studied in this work. The symbol represents a less basic anion while its color indicates the type of the more basic anion for a given binary ionic liquid mixture. For example, filled black triangle refers to $[C_4mim]Cl_x$ $[eFAP]_{1-x}$. Note that open \diamond symbols in orange, violet and magenta colors are three additional ionic liquid mixture systems $[C_4mim][PF_6]_x$ $[NTf_2]_{1-x}$, $[C_4mim][BF_4]_x$ $[NTf_2]_{1-x}$, and $[C_4mim][DCA]_x$ $[NTf_2]_{1-x}$ respectively. Also included is the cation atom numbering used in this work. This figure is best viewed in color. Note that $\delta\beta$ is computed as the difference between the β value for the more basic anion and that for the less basic anion always yielding a positive value. The corresponding absolute value of difference in molar volumes is plotted in the figure.

distribution functions for the binary ionic liquid mixtures of $[C_4mim]Cl_x$ $[NTf_2]_{1-x}$ using an all-atom model in this study vs. a united-atom model in our previous study¹¹ are very similar (see Supporting Information).

Large difference in hydrogen bonding ability and molar volumes lead to non-ideal behavior revealed in terms of non-native microstructures

To rationalize our chosen metrics of ideal vs. non-ideal mixing behavior, we elucidate the composition dependence of the preferential cation–cation and cation–anion interactions by

means of spatial distribution functions (SDFs) of the cation and anions around $[C_4mim]^+$. Figure 2 is one such example for the ionic liquid mixture system of $[C_4mim] Cl_x [eFAP]_{1-x}$ ($\Delta\beta \sim 0.55$ and $\Delta V \sim 218.7 \text{ cm}^3/\text{mol}$ - the highest differences encountered in this work). The general features of SDFs for pure ionic liquid systems share similarities: (i) both anions interact with the cation via acidic ring-hydrogen atoms (H2, H4, and H5 - refer to Figure 1 for the nomenclature); (ii) even though both anions are found in the plane between the two imidazolium rings, the SDFs above and below the plane for the anion with stronger hydrogen bonding interaction are not as extended as those of the weakly coordinating anion. The difference in the spatial extent of the anions enables neighboring cations to participate in $\pi-\pi$ interactions in the presence of a strongly coordinating anion, while a weakly coordinating anion itself establishes anion- π interactions thereby mediating the interactions of two neighboring cations; (iii) The coordination of the anion at the CN3 position (3-methyl position identified in Figure 1) is possible with a strongly coordinating anion; however, the site becomes inaccessible to weakly coordinating anion as shown here and by us and others for different ionic liquid systems.^{11,18,28}

Next, we consider five intermediate mole fractions (0.1, 0.25, 0.5, 0.75, 0.9) for every binary ionic liquid mixture and analyze how the anions distribute around the cation and compare these distributions to those observed for pure ionic liquids. For $[C_4mim] Cl_x [eFAP]_{1-x}$ mixture, even at the lowest Cl^- mole fraction of 0.1, the spatial density localization of Cl^- around the ring-hydrogen atoms begins to resemble that in the pure $[C_4mim] Cl$ system, with a notable exception of the absence of the isosurface density region around CN3 position. This implies that the ring hydrogen sites are the preferred locations for Cl^- and the small addition of Cl^- is effective in displacing the weakly coordinating anion $[eFAP]^-$ from the ring binding sites. Henceforth, we will term such structures as *non-native* structures as they are absent in the pure ionic liquids from which mixtures are generated. The appearance of non-native structure in the SDFs of $[eFAP]^-$ is clearly evident at the Cl^- mole fraction

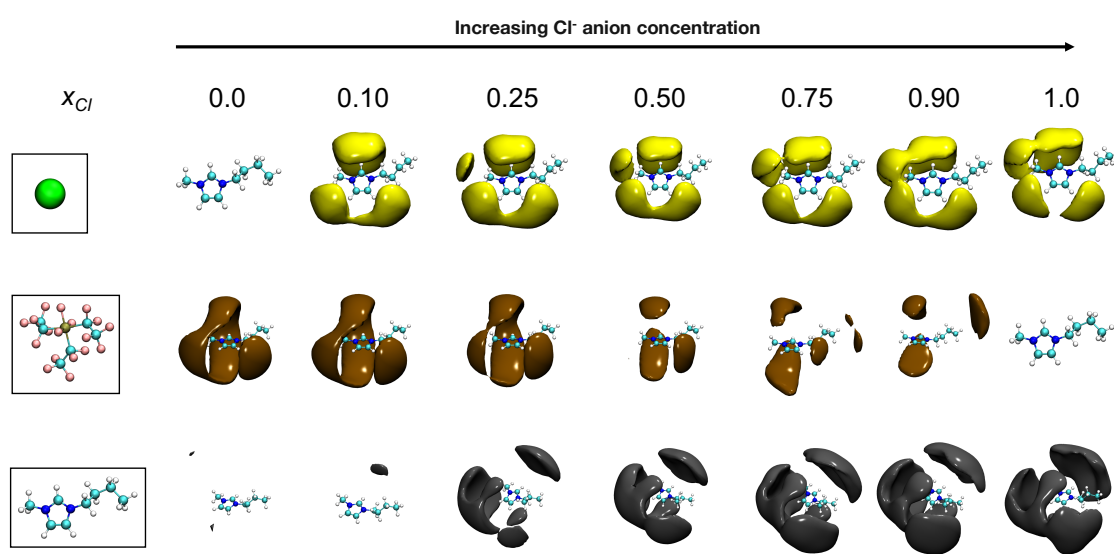


Figure 2: Spatial distribution functions (SDFs) of anions and cation around the cation for the binary ionic liquid mixture of $[\text{C}_4\text{mim}] \text{Cl}_x [\text{eFAP}]_{1-x}$. Isosurface density for cation-anion and cation-cation are 2.5 and 1.5 times the bulk density, respectively. Color coding: Cl^- yellow, $[\text{eFAP}]^-$ golden brown, and $[\text{C}_4\text{mim}]^+$ black. Atoms: C cyan, N blue, H white, O red, S yellow, F orange, and P olive green.

of 0.25 marked by a reduction in the density around the H5 site and thinning of the region connecting the isosurface density regions belonging to H2 and H5. As the mole fraction of Cl^- increases to 0.5, non-native structure is fully established as discerned by the disappearance of the isosurface density from the H5 site and in the plane of the imidazolium ring; $[\text{eFAP}]^-$ is seen to interact with the cation only through the H4 site and above and below the plane of the imidazolium ring through anion- π interactions. With further increase in the Cl^- mole fraction, $[\text{eFAP}]^-$ is prevented from any hydrogen bonding interaction with the cation; the anion- π interactions are retained and surprisingly, new interactions with the butyl chain emerge. The bottom pane in Figure 2 further confirms that cation-cation arrangements (specifically π - π stacking) found in the various mixtures differ from those in the pure ionic liquids at least for Cl^- mole fractions below 0.5.

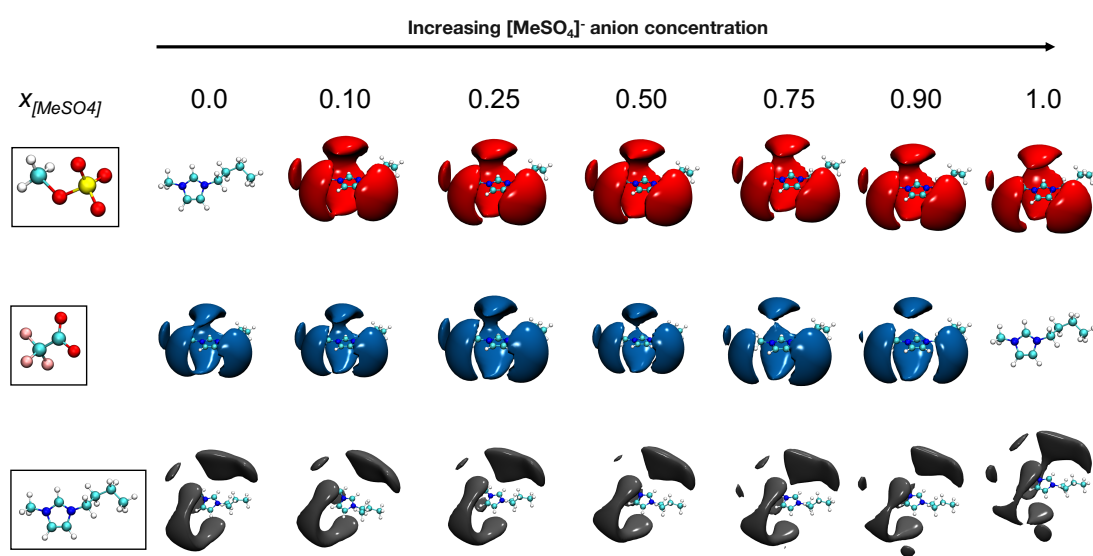


Figure 3: Spatial distribution functions (SDFs) of anions and cation around the cation for the binary ionic liquid mixture of $[\text{C}_4\text{mim}] [\text{MeSO}_4]_x [\text{TFA}]_{1-x}$. Isosurface density for cation-anion and cation-cation are 2.5 and 1.5 times the bulk density, respectively. Color coding: $[\text{MeSO}_4]^-$ red, $[\text{TFA}]^-$ dark blue, and $[\text{C}_4\text{mim}]^+$ black. Atoms: C cyan, N blue, H white, O red, S yellow, F orange, and P olive green.

Small differences in the hydrogen bonding ability and molar volume point to ideal behavior deduced from the absence of non-native molecular structures

The compositional dependence of SDFs for the ionic liquid system $[\text{C}_4\text{mim}] [\text{MeSO}_4]_x [\text{TFA}]_{1-x}$ (Figure 3, $\Delta\beta \sim 0.01$ and $\Delta V \sim 1 \text{ cm}^3/\text{mol}$ – the smallest differences considered in this work) is rather negligible. SDFs indicate that all the favorable sites including CN3 are almost equally accessible to both the anions. Although the density of $[\text{TFA}]^-$ anion in the plane of the imidazolium ring, corresponding to H2 site, vanishes at the $[\text{MeSO}_4]^-$ mole fraction of 0.9, the spatial distribution of $[\text{TFA}]^-$ is almost identical to that for the pure ionic liquid and other mixtures. Furthermore, cation-cation SDFs demonstrate that the $\pi-\pi$ interaction is maintained for all the mixture compositions. In contrast to the $[\text{C}_4\text{mim}] \text{Cl}_x$ $[\text{eFAP}]_{1-x}$ system, we designate the $[\text{C}_4\text{mim}] [\text{MeSO}_4]_x [\text{TFA}]_{1-x}$ system to be an ideal ionic liquid mixture due to the absence of any non-native structures at any composition.

1
2
3 **Radial and angular distribution functions for $[C_4mim]_x [Cl]_{1-x}$ [eFAP]_{1-x} and $[C_4mim]_x [MeSO_4]_{1-x}$ [TFA]_{1-x} systems provide additional means to identify ideal vs. non-ideal**
4 **behavior**
5
6
7
8
9

10 Additional insight into the molecular structures for the two systems discussed above can
11 be gleaned from the radial distribution functions (RDFs) and angular distribution functions
12 (ADFs) provided in the Supporting Information. Akin to the SDFs, a strong composition
13 dependence is seen in the RDFs and ADFs for $[C_4mim]_x [Cl]_{1-x}$ [eFAP]_{1-x} system. An increase
14 in the proportion of strongly coordinating anion (Cl^-) leads to a reduction in the first
15 peak intensity in the cation-Cl and cation-[eFAP] RDFs; the concentration exerts a more
16 pronounced effect on the cation-Cl RDF. The location of the first maximum for cation-[eFAP]
17 RDFs is found to be dependent on the anion composition (except for Cl^- mole fraction of
18 0.9) such that the cation and [eFAP]⁻ are further situated as the Cl^- mole fraction increases;
19 however, the first solvation shell becomes increasingly compact. The observation points to
20 the influence of Cl^- on the cation-[eFAP] interaction, which has the potential to alter the
21 chemical environment around the cation with composition. The shifting of the first peak
22 location appears to be a unique feature of the $[C_4mim]_x [Cl]_{1-x}$ [eFAP]_{1-x} system as the RDFs
23 between the cation and the weakly coordinating anion in the non-ideal mixtures $[C_4mim]_x$
24 $[NTf_2]_{1-x}$ ¹¹ and $[C_4mim]_x [Me_2PO_4]_{1-x}$ $[NTf_2]_{1-x}$ ¹⁸ do not exhibit such compositional
25 dependence. The first solvation shell in the cation-cation RDFs becomes more expanded
26 while the pre-peak shifts to larger distances becoming almost non-existent at high Cl^- is
27 indicative of the disruption of the $\pi-\pi$ interaction. On the other hand, the effect of mixture
28 composition on RDFs and ADFs for $[C_4mim]_x [MeSO_4]_{1-x}$ [TFA]_{1-x} is rather inconspicuous; it
29 appears that the structural transitions can be explained on the basis of simple substitution
30 of one anion by the other.
31
32
33
34
35
36
37
38
39
40
41
42
43
44
45
46
47
48
49
50
51
52
53
54
55
56
57
58
59
60

1
2
3 **The likelihood for the emergence of non-native structure increases for $\Delta\beta > 0.4$.**
4
56 We first discuss four ionic liquid mixtures: $[C_4mim][OAC]_x[TFA]_{1-x}$ ($\Delta\beta \sim 0.11$ and ΔV
7 $\sim 21.1 \text{ cm}^3/\text{mol}$), $[C_4mim][OAC]_x[TFS]_{1-x}$ ($\Delta\beta \sim 0.28$ and $\Delta V \sim 27.8 \text{ cm}^3/\text{mol}$), $[C_4mim]$
8 $[Me_2PO_4]_x[TFA]_{1-x}$ ($\Delta\beta \sim 0.19$ and $\Delta V \sim 25.8 \text{ cm}^3/\text{mol}$), and $[C_4mim][Me_2PO_4]_x[TFS]_{1-x}$
9 ($\Delta\beta \sim 0.36$ and $\Delta V \sim 19.2 \text{ cm}^3/\text{mol}$), where ΔV ranges between $\sim 20\text{-}30 \text{ cm}^3/\text{mol}$ while $\Delta\beta$
10 changes by 3 folds from 0.11 to 0.36 respectively. The SDFs, RDFs, and ADFs for these mix-
11 tures are included in the Supporting Information (Figures S4, S5, S6 and S8 respectively).
12 All the distribution functions are similar to the pure ionic liquid distribution functions, in-
13 dicating that native structures are preserved with the mole fraction. Small deviations from
14 the native structures are obtained for the weakly coordinating fluorinated anions $[TFA]^-$
15 and $[TFS]^-$. For example, the coordination at the H2 position is eliminated when a small
16 amount of $[OAC]^-$ is added to the ionic liquid $[C_4mim][TFA]$ or $[C_4mim][TFS]$. The small
17 non-ideality observed in the $[C_4mim][OAC]_x[TFA]_{1-x}$ system may be a reason that the
18 ionic conductivity of mixtures with $x = 0.1$ and $x = 0.25$ are higher than those for the pure
19 ionic liquid counterparts, while thermophysical properties such as excess molar volumes and
20 self-diffusion coefficients can be approximated with ideal mixing rule.¹⁰ When the strongly
21 coordinating anion is $[Me_2PO_4]^-$, the loss in the interaction of $[TFA]^-$ and the H2 site occurs
22 only at the $[Me_2PO_4]^-$ mole fraction of 0.9. The composition of any of the mixtures does
23 not perturb the cation-cation interactions observed in the corresponding pure ionic liquids.
24 Overall, the four ionic liquid mixtures ($\Delta V_{\max} \sim 30 \text{ cm}^3/\text{mol}$ and $\Delta\beta_{\max} \sim 0.36$) exemplify
25 ideal mixing behavior.
26
2728 To identify the threshold for $\Delta\beta$, we turn our attention to two systems with similar ΔV
29 values but different $\Delta\beta$ such that $\Delta\beta > 0.36$: $[C_4mim]Cl_x[TFS]_{1-x}$ ($\Delta\beta \sim 0.38$ and $\Delta V \sim$
30 $56.0 \text{ cm}^3/\text{mol}$) and $[C_4mim][Me_2PO_4]_x[NTf_2]_{1-x}$ ($\Delta\beta \sim 0.51$ and $\Delta V \sim 48.9 \text{ cm}^3/\text{mol}$). A
31 lack of non-native structures for $[C_4mim]Cl_x[TFS]_{1-x}$ is apparent while non-native struc-
32 tures are clearly seen for $[C_4mim][Me_2PO_4]_x[NTf_2]_{1-x}$ in the SDFs of these systems (Figure
33
34
35
36
37
38
39
40
41
42
43
44
45
46
47
48
49
50
51
52
53
54
55
56
57
58
59
60

S15 and S10, respectively). The findings for these two systems are also consistent with experimental observations by Clough et al.³ that $[C_4mim] Cl_x [TFS]_{1-x}$ mixtures show ideal behavior while $[C_4mim] [Me_2PO_4]_x [NTf_2]_{1-x}$ exhibit non-idealities for a number of physicochemical properties. A similar result was obtained by Matthews et al.¹⁸ experimentally which authors rationalized computationally through SDFs displaying reorganization of the constituent anions. Given that the molar volume differences are nearly identical, the appearance of non-native structures can be entirely ascribed to the greater difference in the $\Delta\beta$ values for $[C_4mim] [Me_2PO_4]_x [NTf_2]_{1-x}$. The absence of non-native structures in $[C_4mim] Cl_x [TFA]_{1-x}$, with similar difference in molar volume ($\Delta V \sim 49.3 \text{ cm}^3/\text{mol}$) and the $\Delta\beta \sim 0.21$ - the smallest of the three ionic liquid mixtures, further substantiates the dominant role difference in hydrogen bonding ability plays in modulating ideal vs. non-ideal behavior. Based on the evidence presented here, we believe that the ionic liquid mixture $[C_4mim] Cl_x [TFS]_{1-x}$ is at the limit of native to non-native structural transition, implying the increasing likelihood of non-ideal behavior as $\Delta\beta$ exceeds 0.4.

Non-native structures become more likely as ΔV increases beyond $60 \text{ cm}^3/\text{mol}$.

We consider two ionic liquid mixtures at roughly identical $\Delta\beta$ and a four-fold increase in ΔV values to determine the threshold for the difference in molar volumes (above) below which the formation of (non-native) native structures can be anticipated: $[C_4mim] [Me_2PO_4]_x [TFS]_{1-x}$ ($\Delta\beta \sim 0.36$ and $\Delta V \sim 19.2 \text{ cm}^3/\text{mol}$) and $[C_4mim] [MeSO_4]_x [NTf_2]_{1-x}$ ($\Delta\beta \sim 0.33$ and $\Delta V \sim 73.7 \text{ cm}^3/\text{mol}$). SDFs in Figures S8 and S17, respectively, convey that the former ionic liquid mixture system is representative of an ideal mixing system, while the latter is that of a non-ideal mixing, suggesting that the threshold for ΔV is between $\sim 20 \text{ cm}^3/\text{mol}$ and $\sim 70 \text{ cm}^3/\text{mol}$. To accurately pinpoint the gap, we turn our attention to three ionic liquids with similar $\Delta\beta$ values but almost a ten-fold increase in the ΔV values: $[C_4mim] [MeSO_4]_x [TFS]_{1-x}$ ($\Delta\beta \sim 0.18$ and $\Delta V \sim 5.6 \text{ cm}^3/\text{mol}$), $[C_4mim] [Me_2PO_4]_x [TFA]_{1-x}$ ($\Delta\beta \sim 0.19$ and $\Delta V \sim 25.8 \text{ cm}^3/\text{mol}$), and $[C_4mim] Cl_x [TFA]_{1-x}$ ($\Delta\beta \sim 0.21$ and $\Delta V \sim 49.4 \text{ cm}^3/\text{mol}$).

The structural information for these ionic liquid mixtures is contained in the Supporting information (Figures S18, S7, and S16, respectively). SDFs for $[C_4mim][MeSO_4]_x[TFS]_{1-x}$ and $[C_4mim][Me_2PO_4]_x[TFA]_{1-x}$ systems show very little dependence with the mole fraction; the only non-native behavior is observed in the form of the elimination of the interaction of the weakly coordinating anion ($[TFS]^-$ or $[TFA]^-$) at high concentrations of $[MeSO_4]^-$ or $[Me_2PO_4]^-$, respectively. Cation-Cl SDFs for $[C_4mim]Cl_x[TFA]_{1-x}$ are identical across the composition range. Some non-ideality, however, is detected in the cation-[TFA] SDFs. For example, the elimination of the in-plane density of TFA occurs at the Cl^- mole fraction of 0.5; however the hydrogen bonding interactions are preserved at the H4 and H5 sites. Thus, it appears that increasing the difference between the molar volumes of ionic liquids begins to manifest in the development of non-native molecular structures, especially for the weakly coordinating anion at increasingly lower concentrations of the anions with stronger hydrogen bonding ability. Collectively, the results for these five systems demonstrate that the critical value for ΔV for separating ideal vs. non-ideal mixing for ionic liquid mixtures is located within $50-70\text{ cm}^3/\text{mol}$ range for a given $\Delta\beta$ value. As a conservative estimate, we establish this limit to be $60\text{ cm}^3/\text{mol}$. The non-native structures, presented in Figure S9, for $[C_4mim][MeSO_4]_x[eFAP]_{1-x}$ ($\Delta\beta \sim 0.35$ and $\Delta V \sim 168.4\text{ cm}^3/\text{mol}$) confirms that a difference in molar volumes greater than $60\text{ cm}^3/\text{mol}$ *will* produce non-ideal behavior.

Non-native structures are produced in ionic liquid mixtures when the limit for ΔV or $\Delta\beta$ is breached.

Furthermore, ionic liquid mixtures of $[C_4mim][Me_2PO_4]_x[NTf_2]_{1-x}$ ($\Delta\beta \sim 0.51$ and $\Delta V \sim 48.9\text{ cm}^3/\text{mol}$), $[C_4mim]Cl_x[NTf_2]_{1-x}$ ($\Delta\beta \sim 0.53$ and $\Delta V \sim 124.0\text{ cm}^3/\text{mol}$) and $[C_4mim][Me_2PO_4]_x[eFAP]_{1-x}$ ($\Delta\beta \sim 0.53$ and $\Delta V \sim 143.6\text{ cm}^3/\text{mol}$) that have similar $\Delta\beta > 0.5$ and have monotonically increasing ΔV also show a non-ideal mixing behavior, with structures comparable to those encountered for $[C_4mim]Cl_x[eFAP]_{1-x}$ ionic liquid mixtures. Our results for $[C_4mim][Me_2PO_4]_x[NTf_2]_{1-x}$ and $[C_4mim]Cl_x[NTf_2]_{1-x}$ are consistent with those

1
2
3 acquired by Matthews et al.¹⁸ using an all-atom model. The large difference in molar volumes
4 of the constituent ionic liquids forming ionic liquid mixtures $[\text{C}_4\text{mim}] [\text{OAC}]_x [\text{NTf}_2]_{1-x}$ ($\Delta\beta$
5 ~ 0.43 and $\Delta V \sim 95.8 \text{ cm}^3/\text{mol}$) and $[\text{C}_4\text{mim}] [\text{OAC}]_x [\text{eFAP}]_{1-x}$ ($\Delta\beta \sim 0.45$ and $\Delta V \sim$
6 $190.5 \text{ cm}^3/\text{mol}$) display non-native structures driven by entropic effects.
7
8
9
10
11

12 Additional Ionic Liquid Systems

13

14
15 As an illustration for the utility of Figure 1, we compare several ionic liquid mixtures
16 for which various physicochemical properties have been measured. The ionic liquid mix-
17 tures tetrafluoroborate $[\text{BF}_4]^-[\text{NTf}_2]$, hexafluorophosphate $[\text{PF}_6]^-[\text{NTf}_2]$ and dicyanamide
18 $[\text{DCA}]^-[\text{NTf}_2]$ shown as open symbols in Figure 1 belong to the class of mixtures in which
19 entropic forces tend to dominate ($\Delta\beta < 0.4$ and $\Delta V > 60 \text{ cm}^3/\text{mol}$). Our classification
20 suggests these ionic liquid mixtures would exhibit non-ideal behavior. Experimental mea-
21 surements of densities and calculations of excess molar volumes by Lopes et al.²⁹ indicate
22 that the mixture systems $[\text{C}_4\text{mim}] [\text{BF}_4]_x [\text{NTf}_2]_{1-x}$ ($\Delta\beta \sim 0.13$, $\Delta V \sim 91.1 \text{ cm}^3/\text{mol}$) and
23 $[\text{C}_4\text{mim}] [\text{PF}_6]_x [\text{NTf}_2]_{1-x}$ ($\Delta\beta \sim 0.02$, $\Delta V \sim 61.1 \text{ cm}^3/\text{mol}$) display positive excess molar
24 volumes; however, the magnitude is higher for the former system reflecting the increase in
25 the non-ideality with the molar volume difference. Larriba et al. demonstrated that the
26 anion pair $[\text{BF}_4]^-$ and $[\text{NTf}_2]^-$, when combined with the cation 1-butylpyridinium $[\text{C}_4\text{pyr}]^+$
27 ($\Delta\beta \sim 0.13$, $\Delta V \sim 108.3 \text{ cm}^3/\text{mol}$), produces non-ideal behavior displayed in the terms of
28 negative deviation for refractive indices and viscosities while positive deviations were found
29 for the excess molar volumes,³⁰ implying that the classification inherent in Figure 1 may
30 be extended to ionic liquid mixtures containing a common cation other than $[\text{C}_4\text{mim}]^+$ as
31 well. Based on the fact that $\Delta\beta$ for the $[\text{DCA}]^-[\text{NTf}_2]$ system is 0.22, higher than that
32 for the $[\text{BF}_4]^-[\text{NTf}_2]$, and the ΔV for both the pairs are nearly identical (ΔV for $[\text{C}_4\text{mim}]$
33 $[\text{DCA}]_x [\text{NTf}_2]_{1-x}$ is $89.5 \text{ cm}^3/\text{mol}$), we predict that $[\text{DCA}]^-[\text{NTf}_2]$ to display non-ideal be-
34 havior. There is no experimental data available for this system, but a similar system of
35 1-propylpyridinium $[\text{C}_3\text{pyr}] [\text{DCA}]^-[\text{NTf}_2]$ investigated by McFarlane and co-workers³¹ was
36
37
38
39
40
41
42
43
44
45
46
47
48
49
50
51
52
53
54
55
56
57
58
59
60

1
2
3 found to be non-ideal. Thus, it is conceivable that the $[DCA]-[NTf_2]$ would be classified
4 as an example of a non-ideal mixture system. Likewise, a large difference in the hydrogen
5 bonding ability of anions can form non-ideal mixtures even if the difference in molar volumes
6 is small, as already demonstrated for $[C_4mim][Me_2PO_4]_x[NTf_2]_{1-x}$ ($\Delta\beta > 0.4$ and $\Delta V < 60$
7 cm^3/mol). The conclusion derived here suggests that the ionic liquid mixture 1-*n*-butyl-
8 methylpyrrolidinium $[C_4C_1pyrr][Me_2PO_4]_x[NTf_2]_{1-x}$ is likely to exhibit non-ideal behavior,
9 which is in line with experimental observation³ of non-ideal behavior across a range of prop-
10 erties such as excess molar volumes, viscosity, conductivity, and glass transition temperature
11 with either $[C_4mim]^+$ or $[C_4C_1pyrr]^+$ cations paired with the two anions. The substan-
12 tial difference in the hydrogen bonding ability between ethylsulfate $[C_2SO_4]^-$ and $[NTf_2]^-$
13 ($\Delta\beta \sim 0.35$) with $[C_2mim]^+$ ($\Delta V \sim 60 cm^3/mol$ at 298.15 K and 1 bar) results in a more
14 pronounced ¹H NMR shift for the acidic hydrogen as the concentration of $[C_2mim][C_2SO_4]$
15 increases, indicating preferential interaction of $[C_2SO_4]^-$ with the cation. On the other hand,
16 only marginal chemical shifts are recorded when mixtures comprised of anions with similar
17 hydrogen bonding ability are probed, e.g. $[C_2mim][C_2SO_4]_x[CF_3SO_3]_{1-x}$ ($\Delta\beta \sim 0.2$ and
18 $\Delta V \sim 45 cm^3/mol$) and $[C_2mim][C_2SO_4]_x$ thiocyanate $[SCN]_{1-x}$ ($\Delta\beta \sim 0.06$ and $\Delta V \sim 65$
19 cm^3/mol);³² the trends correspond to the characteristics of the regions these ionic liquid
20 mixture are located in.
21
22
23
24
25
26
27
28
29
30
31
32
33
34
35
36
37
38
39
40
41
42
43
44
45
46
47
48
49
50
51
52
53
54
55
56
57
58
59
60

The general applicability of Figure 1 for predicting non-ideal behavior can be further demonstrated using a contrived example of the ionic liquid mixtures containing a common anion ($\Delta\beta \sim 0$) as in 1-ethyl-3-methylimidazolium $[C_2mim]^+$ and 1-*n*-octyl-3-methylimidazolium $[C_8mim]^+$ combined with $[BF_4]^-$ ($\Delta V \sim 100 cm^3/mol$) at 298.15 K. The binary mixtures have been recently reported to exhibit non-ideal behavior reflected in terms of dielectric constants; for few mixture compositions, the dielectric constant was almost a factor of two higher than those for the pure ionic liquids.³³ Although the molecular-level explanation of the non-ideal behavior is completely different from that used to identify non-native struc-

tures here, Figure 1 proves to be a useful guide for predicting the non-ideality. Along these lines, we can scrutinize three ionic liquid mixtures containing the common anion $[\text{NTf}_2]^-$ but different cations: $[\text{C}_2\text{mim}]^+$ and 1-*n*-decyl-3-methylimidazolium $[\text{C}_{10}\text{mim}]^+$, $[\text{C}_2\text{mim}]^+$ and 1-*n*-hexyl-3-methylimidazolium $[\text{C}_6\text{mim}]^+$, and $[\text{C}_4\text{mim}]^+$ and $[\text{C}_6\text{mim}]^+$. The non-ideality expressed in terms of ^{129}Xe NMR chemical shifts for the first two ionic liquid mixtures were observed to be much more pronounced than those for the third ionic liquid mixture.³⁴ This observation correlates very well with the guidance provided from Figure 1 as the ΔV values are $\sim 141 \text{ cm}^3/\text{mol}$, $106 \text{ cm}^3/\text{mol}$, and $35 \text{ cm}^3/\text{mol}$, respectively, based on the densities of the ionic liquids reported at 323 K ($\Delta\beta \sim 0$ for all the ionic liquids).³⁵

Conclusion

Molecular dynamics simulations were conducted for a total of sixteen ionic liquid mixtures comprising of the cation $[\text{C}_4\text{mim}]^+$ and a combination of anions enabling us to vary the enthalpic and entropic contributions through the difference in the hydrogen bonding ability of the anions and ionic liquid molar volumes, respectively. Distributions of anions around the cation and their deviation from those in the pure ionic liquids making up a given mixture were employed to quantify the non-ideality of the mixture. A considerable imbalance in the enthalpic and entropic effects reflected in terms large differences in molar volumes and hydrogen bonding ability of anions ($\Delta V > 60 \text{ cm}^3/\text{mol}$ and $\Delta\beta > 0.4$) translated into anion distributions that differed markedly from those in the corresponding pure ionic liquids. Specifically, the anion with weaker hydrogen bonding ability lost its favorable interaction with the ring hydrogen atoms, resulting in its occupying positions above and below the plane of the imidazolium ring. The rearrangement induced a disruption in the π - π stacking of the two neighboring cations, leading to the observation of structures non-native to those in the parent ionic liquids. We also illustrated that non-native structures could arise in ionic liquid mixtures even when a large difference exists in only one of the descriptors. On the other hand,

1
2
3 small differences in both the descriptors led to minimal deviation of ionic arrangements for
4 ionic liquid mixtures. The identification of regions demarcated by the values of ΔV and $\Delta\beta$
5 has the potential to serve as a useful guide to quickly screen emergent ionic liquid mixtures
6 for non-ideal physicochemical properties.
7
8
9
10

11 12 13 Acknowledgement 14

15
16 This material is based upon work supported by the National Science Foundation (NSF)
17 Award Number CBET-1706978. The authors gratefully acknowledge partial funding from
18 the Oklahoma State University. Computational resources were provided by the High Perfor-
19 mance Computing Center (HPCC) at the Oklahoma State University.
20
21
22
23

24 25 26 Supporting Information Available 27 28

29
30 Supporting information includes force field and simulation details along with RDFs, SDFs
31 and ADFs of 16 binary ionic liquid mixtures studied in this work. This material is available
32 free of charge via the Internet at <http://pubs.acs.org/>.
33
34

35 36 37 38 References 39

40
41 (1) Chatel, G.; Pereira, J. F. B.; Debbeti, V.; Wang, H.; Rogers, R. D. Mixing Ionic Liquids
42 – “Simple Mixtures” or “Double Salts”? *Green Chem.* **2014**, *16*, 2051–33.
43
44 (2) Niedermeyer, H.; Hallett, J. P.; Villar-Garcia, I. J.; Hunt, P. A.; Welton, T. Mixtures
45 of Ionic Liquids. *Chem. Soc. Rev.* **2012**, *41*, 7780–23.
46
47 (3) Clough, M. T.; Crick, C. R.; Gräsvik, J.; Hunt, P. A.; Niedermeyer, H.; Welton, T.;
48 Whitaker, O. P. A Physicochemical Investigation of Ionic Liquid Mixtures. *Chem. Sci.*
49
50 **2014**, *00*, 1–14.
51
52
53
54
55
56
57
58

1
2
3 (4) Hayes, R.; Warr, G. G.; Atkin, R. Structure and Nanostructure in Ionic Liquids. *Chem.*
4 *Rev.* **2015**, *115*, 6357–6426.

5
6 (5) Lei, Z.; Dai, C.; Chen, B. Gas Solubility in Ionic Liquids. *Chem. Rev.* **2013**, *114*,
7 1289–1326.

8
9 (6) Sivapragasam, M.; Moniruzzaman, M.; Goto, M. Recent advances in exploiting ionic
10 liquids for biomolecules: Solubility, stability and applications. *Biotechnology Journal*
11 **2016**, *11*, 1000–1013.

12
13 (7) Watanabe, M.; Thomas, M. L.; Zhang, S.; Ueno, K.; Yasuda, T.; Dokko, K. Application
14 of Ionic Liquids to Energy Storage and Conversion Materials and Devices. *Chem. Rev.*
15 **2017**, *117*, 7190–7239.

16
17 (8) Dong, K.; Liu, X.; Dong, H.; Zhang, X.; Zhang, S. Multiscale Studies on Ionic Liquids.
18 *Chem. Rev.* **2017**, *117*, 6636–6695.

19
20 (9) Plechkova, N. V.; Seddon, K. R. Applications of Ionic Liquids in the Chemical Industry.
21 *Chem. Soc. Rev.* **2008**, *37*, 123–150.

22
23 (10) Kapoor, U.; Shah, J. K. Thermophysical Properties of Imidazolium-Based Binary Ionic
24 Liquid Mixtures Using Molecular Dynamics Simulations. *J. Chem. Eng. Data* **2018**,
25 *63*, 2512–2521.

26
27 (11) Kapoor, U.; Shah, J. K. Preferential Ionic Interactions and Microscopic Structural
28 Changes Drive Nonideality in Binary Ionic Liquid Mixtures as Revealed from Molecular
29 Simulations. *Ind. Eng. Chem. Res.* **2016**, *55*, 13132–13146.

30
31 (12) Kapoor, U.; Shah, J. K. Molecular Origins of the Apparent Ideal CO₂ Solubilities in
32 Binary Ionic Liquid Mixtures. *J. Phys. Chem. B* **2018**, *122*, 9763–9774.

33
34 (13) Canongia Lopes, J. N.; Pádua, A. A. H. Molecular Force Field for Ionic Liquids

35
36
37
38
39
40
41
42
43
44
45
46
47
48
49
50
51
52
53
54
55
56
57
58
59
60

1
2
3 III: Imidazolium, Pyridinium, and Phosphonium Cations; Chloride, Bromide, and
4 Dicyanamide Anions. *J. Phys. Chem. B* **2006**, *110*, 19586–19592.
5
6 (14) Canongia Lopes, J. N.; Pádua, A. A. H.; Shimizu, K. Molecular Force Field for Ionic
7 Liquids IV: Trialkylimidazolium and Alkoxycarbonyl-Imidazolium Cations; Alkylsul-
8 fonate and Alkylsulfate Anions. *J. Phys. Chem. B* **2008**, *112*, 5039–5046.
9
10 (15) Jorgensen, W. L.; Maxwell, D. S.; Tirado-Rives, J. Development and Testing of the
11 OPLS All-Atom Force Field on Conformational Energetics and Properties of Organic
12 Liquids. *J. Am. Chem. Soc.* **1996**, *118*, 11225–11236.
13
14 (16) Niazi, A. A.; Rabideau, B. D.; Ismail, A. E. Effects of Water Concentration on the
15 Structural and Diffusion Properties of Imidazolium-Based Ionic Liquid–Water Mixtures.
16 *J. Phys. Chem. B* **2013**, *117*, 1378–1388.
17
18 (17) Rabideau, B. D.; Ismail, A. E. Mechanisms of hydrogen bond formation between ionic
19 liquids and cellulose and the influence of water content. *Phys. Chem. Chem. Phys.*
20 **2015**, *17*, 5767–5775.
21
22 (18) Matthews, R. P.; Villar-Garcia, I. J.; Weber, C. C.; Griffith, J.; Cameron, F.; Hal-
23 lett, J. P.; Hunt, P. A.; Welton, T. A Structural Investigation of Ionic Liquid Mixtures.
24 *Phys. Chem. Chem. Phys.* **2016**, *18*, 8608–8624.
25
26 (19) Yan, T.; Wang, Y.; Knox, C. On the Structure of Ionic Liquids: Comparisons between
27 Electronically Polarizable and Nonpolarizable Models I. *J. Phys. Chem. B* **2010**, *114*,
28 6905–6921.
29
30 (20) Lindahl, E.; Hess, B.; van der Spoel, D. GROMACS 3.0: A Package for Molecular
31 Simulation and Trajectory Analysis. *Molec. Model. Ann.* **2001**, *7*, 306–317.
32
33 (21) Abraham, M. J.; van der Spoel, D.; Lindahl, E.; Hess, B.; ; the GROMACS development
34 team, GROMACS User Manual Version 5.1.4, www.gromacs.org. *J. Mol. Model.* **2014**,

(22) Martínez, L.; Andrade, R.; Birgin, E. G.; Martínez, J. M. PACKMOL: A Package for Building Initial Configurations for Molecular Dynamics Simulations. *J. Comput. Chem.* **2009**, *30*, 2157–2164.

(23) Brehm, M.; Kirchner, B. TRAVIS - A Free Analyzer and Visualizer for Monte Carlo and Molecular Dynamics Trajectories. *J. Chem. Inf. Model.* **2011**, *51*, 2007–2023.

(24) Lungwitz, R.; Spange, S. A Hydrogen Bond Accepting (HBA) Scale For Anions, Including Room Temperature Ionic Liquids. *New J. Chem.* **2008**, *32*, 392–3.

(25) Lungwitz, R.; Strehmel, V.; Spange, S. The Dipolarity/Polarisability of 1-Alkyl-3-Methylimidazolium Ionic Liquids as Function of Anion Structure and The Alkyl Chain Length. *New J. Chem.* **2010**, *34*, 1135–6.

(26) Cláudio, A. F. M.; Swift, L.; Hallett, J. P.; Welton, T.; Coutinho, J. A. P.; Freire, M. G. Extended Scale for Hydrogen-Bond Basicity of Ionic Liquids. *Phys. Chem. Chem. Phys.* **2014**, *16*, 5975–5984.

(27) Ab Rani, M. A.; Brant, A.; Crowhurst, L.; Dolan, A.; Lui, M.; Hassan, N. H.; Hallett, J. P.; Hunt, P. A.; Niedermeyer, H.; Perez-Arlandis, J. M. et al. Understanding The Polarity of Ionic Liquids. *Phys. Chem. Chem. Phys.* **2011**, *13*, 16831–10.

(28) Payal, R. S.; Balasubramanian, S. Homogenous mixing of ionic liquids: molecular dynamics simulations. *Phys. Chem. Chem. Phys.* **2013**, *15*, 21077–7.

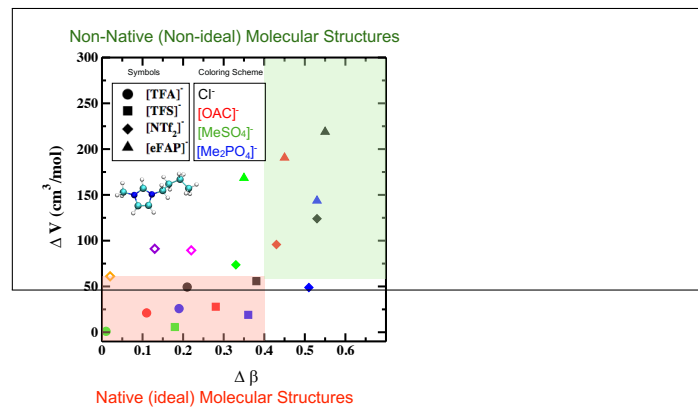
(29) Canongia Lopes, J. N.; Cordeiro, T. C.; Esperança, J. M. S. S.; Guedes, H. J. R.; Huq, S.; Rebelo, L. P. N.; Seddon, K. R. Deviations from Ideality in Mixtures of Two Ionic Liquids Containing a Common Ion. *J. Phys. Chem. B* **2005**, *109*, 3519–3525.

(30) Larriba, M.; García, S.; Navarro, P.; García, J.; Rodríguez, F. Physical Properties of N-Butylpyridinium Tetrafluoroborate and N-Butylpyridinium

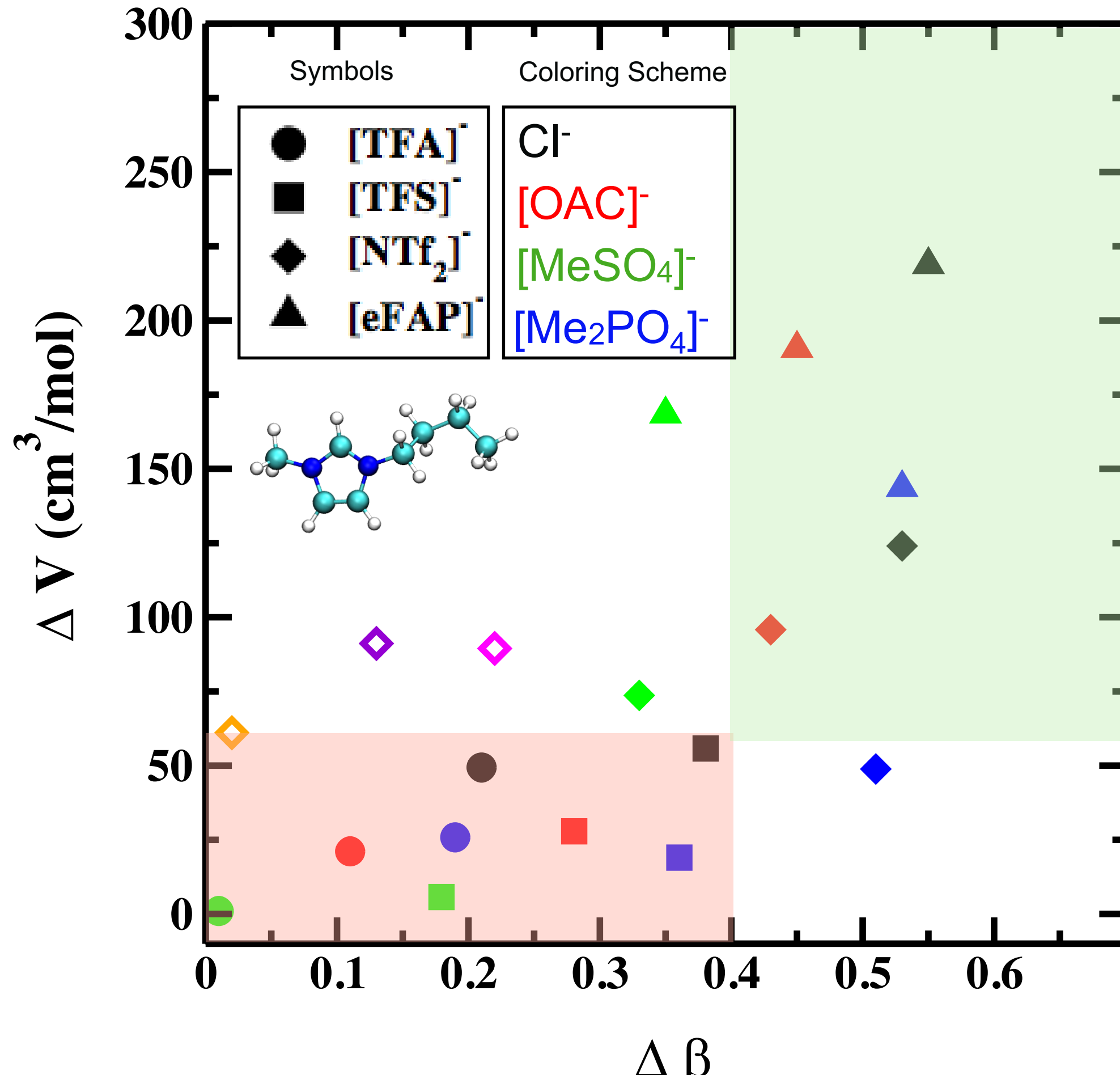
1
2
3 Bis(trifluoromethylsulfonyl)imide Binary Ionic Liquid Mixtures. *J. Chem. Eng. Data*
4
5 **2012**, *57*, 1318–1325.
6
7

8 (31) Annat, G.; Forsyth, M.; MacFarlane, D. R. Ionic Liquid Mixtures—Variations in Phys-
9 ical Properties and Their Origins in Molecular Structure. *J. Phys. Chem. B* **2012**, *116*,
10 8251–8258.
11
12 (32) Ijardar, S. P.; Saparov, A.; Shah, D. Insights into Non-Ideal Behavior of Double Salt
13 Ionic Liquids with Common Cation: Volumetric Behaviour, Molecular Dynamics Sim-
14 ulations and NMR Experiments. *ChemistrySelect* **2019**, *4*, 12861–12870.
15
16 (33) Cosby, T.; Kapoor, U.; Shah, J. K.; Sangoro, J. Mesoscale Organization and Dynamics
17 in Binary Ionic Liquid Mixtures. *arXiv e-prints* **2019**, arXiv:1905.02827.
18
19 (34) Weber, C. C.; Brooks, N. J.; Castiglione, F.; Mauri, M.; Simonutti, R.; Mele, A.;
20 Welton, T. On the structural origin of free volume in 1-alkyl-3-methylimidazolium ionic
21 liquid mixtures: a SAXS and ¹²⁹Xe NMR study. *Physical Chemistry Chemical Physics*
22 **2019**, *21*, 5999–6010.
23
24 (35) Tariq, M.; Forte, P. A. S.; Gomes, M. F. C.; Lopes, J. N. C.; Rebelo, L. P. N. Densities
25 and refractive indices of imidazolium- and phosphonium-based ionic liquids: Effect of
26 temperature, alkyl chain length, and anion. *Journal of chemical thermodynamics* **2009**,
27 *41*, 790–798.
28
29
30
31
32
33
34
35
36
37
38
39
40
41
42
43
44
45
46
47
48
49
50
51
52
53
54
55
56
57
58
59
60

Graphical TOC Entry



Non-Native (Non-ideal) Molecular Structures



Native (ideal) Molecular Structures

ACS Paragon Plus Environment